Ocean Sci. Discuss., https://doi.org/10.5194/os-2017-38
Manuscript under review for journal Ocean Sci.
Discussion started: 11 July 2017

Ocean Science Discussions

An Undercurrent off the East Coast of Sri Lanka

Arachaporn Anutaliya[1], Uwe Send[1], Julie L, McClean[1], Janet Sprintall[1], Luc Rainville[2], Craig Lee[2], S. U. Prinyatha Jinadasa[3], Alan J. Wallcraft[4], E. Joseph Metzger[4]

[1]Scripps Institution of Oceanography, La Jolla, California, USA
[2]Applied Physics Laboratory, University of Washington, Seattle, Washington, USA
[3]National Aquatic Resources Research and Development Agency, Colombo, Sri Lanka
[4]Naval Research Laboratory, Stennis Space Center, Mississippi, USA

Correspondence to: Arachaporn Anutaliya (aanutali@ucsd.edu)

Abstract. The existence of a seasonally varying undercurrent along 8° N off the east coast of Sri Lanka is inferred from Conductivity-Temperature-Depth profiles, Argo floats, glider measurements, and Ocean General Circulation Model outputs. Together, they reveal an undercurrent below 200 m that is approximately 140 km wide and can reach a maximum speed of 45 cm s^{-1} that hitherto has not been observed. The undercurrent, flowing in the opposite direction to the surface current, is most pronounced during boreal spring and summer and switches direction between these two seasons. The undercurrent transports relatively fresh water southward during spring, while it advects more saline water northward along the east coast of Sri Lanka during summer. This suggests a pathway, independent of the surface circulation, whereby freshwater is removed and saline water is injected into the Bay of Bengal.

1 Introduction

Knowledge of the circulation in the southern Bay of Bengal (BoB) is crucial to understanding the contrasting salinity distributions of the Arabian Sea (AS) and the BoB since it determines the amount of water and salt exchanged between the two ocean basins. Observations and model studies have confirmed the role of the surface current along the Sri Lankan east coast in distributing mass and salt between the AS and the BoB. Drifters indicate that a strong surface-intensified current to the east of Sri Lanka during the northeast monsoon (boreal winter) transports low-salinity water out of the BoB toward the AS around the south coast of Sri Lanka (Wijesekera et al., 2015). A numerical ocean model study also shows that significant mass and salt transport occurs between the AS and the BoB along the east and south coast of Sri Lanka (Jensen et al., 2016).

The surface current to the east of Sri Lanka is influenced by local alongshore winds, remote winds in the vicinity of the northern and eastern boundaries of the BoB, equatorial waves, and interior Ekman pumping (Yu et al., 1991; Shetye et al., 1993; McCreary et al., 1996; Shankar et al., 1996; Vinayachandran et al., 1997). This current has a strong seasonal pattern (Lee et al., 2016) with recirculation loops that are highly variable in time and space (Durand et al., 2009). Some of the recirculations appear seasonally, such as the Sri Lanka Dome (SLD), a cyclonic eddy that is well-developed in July (Vinayachandran et al., 1997). As it is being driven by Rossby waves radiating from the eastern boundary and intensified Ekman pumping inside the BoB (Vinayachandran et al., 1999; de

Ocean Sci. Discuss., https://doi.org/10.5194/os-2017-38
Manuscript under review for journal Ocean Sci.
Discussion started: 11 July 2017

Vos et al., 2014), the SLD propagates westward until it approaches the east coast of Sri Lanka yielding a coastal surface flow that is southward during early summer and northward during late summer. In October, the prevailing wind in the BoB starts reversing direction and blows southwestward. This marks the start of the northeast monsoon when the local wind along the east coast of India drives the East India Coastal Current (EICC) southward with speeds exceeding 1 m s^{-1} extending from the east coast of India southward to the southern tip of Sri Lanka (Shetye et al., 1996; Wijesekera et al., 2015).

Little is known about the subsurface structure of the boundary current to the east of Sri Lanka. Yet, the subsurface circulation is also important as high-salinity water from the AS can be subducted beneath the fresher surface water originating from river runoff and precipitation in the northern BoB (Rao & Sivakumar, 2003; Sengupta et al., 2006; Vinayachandran et al., 2013; Gordon et al., 2016; Jensen et al., 2016). Observations and model studies (Wijesekera et al., 2015) show a shallow subsurface current over the 50-75 m layer in the southern BoB, between 82.5°E and 85°E, during the northeast monsoon that transports saline water into the BoB. A linear, continuously stratified ocean model (McCreary et al., 1996) suggests that westward propagating Rossby waves and interior Ekman pumping in the BoB can produce significant subsurface flow off the east coast of Sri Lanka. Their modeling study suggests the existence of a subsurface current flowing in the opposite direction to the surface current across 8° N that can be as strong as 30 cm s^{-1} and extends from 200 to deeper than 1000 m depth. However, due to sparse measurements in this region, the subsurface current has not yet been observed and the vertical structure of the boundary current is not well understood.

The purpose of this study is to investigate the vertical structure and seasonal variability of subsurface flows in the boundary current system to the east of Sri Lanka using Ocean General Circulation Models (OGCMs) as well as observations from Conductivity-Temperature-Depth (CTD), Argo floats, and glider measurements. Knowledge of the vertical structure, variability, and associated dynamics of the boundary current will provide a better understanding of salt and mass exchanges in the northern Indian Ocean.

2 Data and Methodology

CTD and Argo profiles, together with satellite surface absolute dynamic topography (ADT), were used to determine the vertical structure of the current east of Sri Lanka. There were 54 CTD and 20 Argo profiles available between 7-9° N and within 130 km of the Sri Lankan east coast (Figure 1a). The CTD profiles were sampled over the period of 1961- 2011 while the Argo profiles were collected over 2005-2016. The gridded delayed-time ADT products were derived from Archiving, Validation, and Interpretation of Satellite Oceanographic (AVISO) Data (Ducet et al., 2000) which are available over 1993-2016 with spatial and temporal resolutions of ¼° latitude × ¼° longitude and 7 days, respectively.

The mean seasonal meridional velocity profiles were calculated by combining sheared velocity profiles from CTD and Argo measurements and surface velocity from the ADT products. To derive the seasonal sheared velocity profiles, bimonthly sliding mean dynamic heights from CTD profiles were calculated

Ocean Sci. Discuss., https://doi.org/10.5194/os-2017-38
Manuscript under review for journal Ocean Sci.
Discussion started: 11 July 2017

positioned east, within 50 km from the coast, and west, between 50-130 km from the coast, of the expected central position of the boundary current. The number of CTD and Argo profiles available in each bimonthly period varied from 3 to 6 in the western region and from 3 to 16 in the eastern region (Figure 1b). The bimonthly mean geostrophic meridional sheared velocity profile is proportional to the corresponding difference between the eastern and western mean bimonthly dynamic heights. Adding the bimonthly mean surface meridional velocity from the satellite ADT along 8° N between 81.75° E-82.5° E to the sheared profiles yielded bimonthly absolute geostrophic meridional velocity profiles.

Gliders were deployed to the east of Sri Lanka between 7° N and 9° N to collect salinity and temperature measurements from the surface to 1000 m depth since February 2014 (Lee et al., 2016) (Figure 1a). Temperature and salinity profiles collected from gliders during February 2014–January 2016 were used in the same way as the CTD and Argo profiles to calculate bimonthly sliding mean geostrophic meridional velocity. Absolute geostrophic velocity is obtained by referencing the profile to the depth-averaged velocity.

Two OGCMs were used to study the seasonal variation of the boundary current and the associated dynamics: 0.1° global Parallel Ocean Program (POP) and 0.08° global HYbrid Coordinate Ocean Model (HYCOM). Their horizontal resolutions correspond to 11 km and 9 km at 8°N, respectively. POP is a three-dimensional, z-level, primitive equation model (Smith et al., 2010). It was configured on a global tripole grid with 42 vertical levels. Vertical spacing near the surface is roughly 10 m. The simulation analyzed in this study was initialized from Year 30 of an earlier POP simulation run on this same grid and driven by a monthly climatology of Co-ordinated Ocean Reference Experiments (CORE) atmospheric surface fluxes (Maltrud et al., 2010). Our analysis run was forced by interannually-varying CORE-II fluxes for 1990-2007 (Delman et al., 2015). POP output analyzed here are three-dimensional daily-averaged velocities and salinity for 1995-2007. HYCOM has a hybrid vertical coordinate with isopycnal coordinates in the open stratified ocean, a terrain-following coordinate for coastal regions, and a z-level coordinate in the mixed layer (Metzger et al., 2010). It was configured on a global tripole grid with 41 vertical layers. Vertical spacing near the surface is roughly 1 m. The simulation was forced by 3 hourly Navy Operational Global Forecasting Prediction System (NOGAPS) atmospheric forcing (Rosmond et al., 2002). However, the archived velocity fields used here are monthly and cover a shorter period compared to POP of 2003-2012.

3 The Circulation east of Sri Lanka

An undercurrent is defined here as the maximum velocity core of the subsurface flow that is separated from the surface current by weak flow. Unambiguous cases exist when the subsurface flow is in the opposite direction to the surface flow. This is clearly observed in longitude-depth transects of absolute geostrophic meridional velocities across 8° N derived from glider measurements and meridional velocities from the OGCMs (Figure 2). Glider geostrophic velocities were from measurements during March 18-30, 2014 (Figure 2a) and May 28–June 8, 2014 (Figure 2d) and velocity transects from HYCOM (Figure 2b,e) and POP (Figure 2c,f) are the monthly averages in March and June for the

periods of 2003-2012 and 1995-2007, respectively. The transects show good agreement in vertical structure, width, and intensity of both the surface current and undercurrent. The glider velocity transect in March 2014 shows the expected northward-flowing surface current along the east coast of Sri Lanka which is confined to the top 200 m of the water column (Figure 2a). This boundary current reverses its direction below 200 m with a subsurface velocity maximum core found below 800 m and a maximum speed greater than 25 cm s^{-1}. Both velocity transects from the OGCMs show similar results to the observations, except that the model mean surface current extends to approximately 100 m and the subsurface velocity maximum core is located between 400-600 m (Figure 2b,c). In June, both glider and OGCM results show the expected strong southward surface current in the 0-200 m layer (Figure 2d-f). A northward undercurrent is apparent at this time below 200 m with its maximum speed greater than 20 cm s^{-1} at about 800 m. During March and June, the undercurrent is confined to the west of 82.5° E and is approximately 85 km wide.

Bimonthly mean meridional velocities, computed from CTD and Argo profiles and glider measurements, are shown in Fig. 3a and b respectively. Monthly mean meridional velocities were constructed from the OGCMs by averaging the monthly mean velocity across 8° N over the width of the undercurrent between 81.75° E and 82.5° E (depicted by the magenta transect in Fig. 1) (Figure 3c,d).

Both surface and subsurface currents have strong seasonal variability (Figure 3). The surface current reverses its direction four times a year in agreement with previous studies (Yu et al., 1991; McCreary et al., 1996; Shetye et al., 1996; Vinayachandran et al., 1997; Vinayachandran et al., 1999; Durand et al., 2009; Wijesekera et al., 2015; Lee et al., 2016). An undercurrent flowing in the opposing direction to the surface current is a prominent and consistent feature among the observations and OGCMs in boreal spring (March-April) and summer (June-July).

The mean meridional surface current is northward with speeds exceeding 10 cm s^{-1} during boreal spring (Figure 3) in good agreement with that derived from the satellite altimetry (Lee et al., 2016). The westward flowing North Equatorial Current is dominant at the surface in this season; it often bifurcates at the east coast of Sri Lanka splitting into a northward and southwestward branch at approximately 7.5° N resulting in a northward surface current along the east coast (Shetye et al., 1993; Hacker et al., 1998; de Vos et al., 2014). The velocity derived from CTD and Argo profiles and glider measurements confirm the existence of the undercurrent below 150 m (Figure 3a,b). The southward-flowing undercurrent is the strongest during March-April. Mean velocity profiles derived from the observations and the OGCMs agree that the core of the undercurrent is between 300-400 m depth. The CTD and Argo-derived velocity shows that the mean undercurrent can reach nearly 50 cm s^{-1} at 300 m. At 729 m depth, the POP velocity fields show a strong and confined southward undercurrent along the entire east coast (Movie S1). Figure 4a shows a simplified schematic of the undercurrent during boreal spring that usually turns eastward around 6° N to combine with an eastward-flowing current along the south coast from the AS. However, in some years (e.g. 1995, 1999, 2005, and 2007), the undercurrent turns westward around the southern tip of Sri Lanka and forms a narrow current, about 50-70 km wide, on the northern side of the eastward flow (Movie S1).

Ocean Sci. Discuss., https://doi.org/10.5194/os-2017-38
Manuscript under review for journal Ocean Sci.
Discussion started: 11 July 2017

During the boreal summer, the surface current, which forms as a western branch of the SLD, is southward and has a mean speed as high as 40 cm s^{-1}, while the northward-flowing undercurrent is found below approximately 200 m (Figure 3). The observations and OGCMs agree that the undercurrent starts developing in May and reaches a maximum speed during June-July with a core at 800 m. The maximum mean speed can be as strong as 35 cm s^{-1} (Figure 3). In early summer, the POP velocity fields show a convergence of the eastward-flowing current along the south coast of Sri Lanka and a southwestward-flowing current in the southeast BoB at approximately 7° N and 82.25° E as shown in a simplified schematic (Figure 4b). Both OGCMs agree that the convergence produces the undercurrent flowing north along the east coast of Sri Lanka that injects relatively saline water into the BoB. Also, an anticyclonic eddy usually develops along the east coast, trapping local saline water inside, which is then propagated northward with the eddy (Movie S1).

The glider-derived velocity over the 2014-2016 period shows strong northward and southward flows in the surface and subsurface layers during boreal fall (Figure 3b); the subsurface current can reach 20 cm s^{-1} at 1000 m. However, this feature might not be persistent across the years; the velocity profiles derived from the OGCMs and the CTD and Argo profiles show a weak northward-flowing surface current and a weak southward-flowing subsurface current during boreal fall (Figure 3a,c,d). The subsurface current has a maximum mean speed of 5-10 cm s^{-1} at 500-750 m depth, according to the CTD and Argo-derived velocity and the OGCMs. Standard deviation of meridional velocity across 8° N during fall derived from HYCOM and CTD and Argo profiles (9.4 cm s^{-1} and 54 cm s^{-1}) is higher than the mean (-6.8 cm s^{-1} and -11 cm s^{-1}) over the 200-1000 m layer. Also, longitude-depth transects of meridional velocity across 8° N in boreal fall from POP and HYCOM (not shown) do not show a well-defined undercurrent near the east coast of Sri Lanka in the top 1000 m of the water column.

During boreal winter, the surface flow is southward and stronger than 40 cm s^{-1} (Figure 3). The seasonal mean subsurface current derived from CTD and Argo profiles is northward in contrast to that derived from the OGCMs and the gliders; the disagreement might arise from the small number of CTD and Argo profiles used in the velocity calculation during boreal winter (Figure 1b). The glider-derived velocity of the subsurface current is much stronger than that from the OGCMs. Since glider measurements cover the period of 2014-2016, the inconsistency suggests high variability of the subsurface current from year to year. The CTD-and-Argo-derived and the HYCOM velocity profiles also suggest that the interannual variation of the subsurface current is high; the standard deviation of the velocity below 200 m across 8°N (56 cm s^{-1} and 8.1 cm s^{-1}) is roughly twice as large as its mean (17 cm s^{-1} and -4.2 cm s^{-1}) during the winter. Moreover, the current at 729 m in the POP winter velocity fields appears as a transient current rather than a seasonal undercurrent (Movie S1). More observations are needed to understand the vertical structure and the associated dynamics of the subsurface boundary current during the winter.

Ocean Sci. Discuss., https://doi.org/10.5194/os-2017-38
Manuscript under review for journal Ocean Sci.
Discussion started: 11 July 2017

4 Discussion

The undercurrent potentially plays an important role in salt and mass exchange between the AS and the BoB as suggested by the velocity fields of the OGCM. During the summer, the undercurrent injects relatively saline water into the western boundary of the BoB that can be trapped in a northward-propagating seasonal anticyclonic eddy (Figure 4b and Movie S1). Relatively freshwater is transported southward along the east coast of Sri Lanka in the subsurface layer in spring (Figure 4a). It can be advected westward along the Sri Lankan south coast in some years depending on the strength and location of the eastward flowing current along the south coast (Movie S1). The POP velocity fields further reveal that the zonal current along the south coast of Sri Lanka is the strongest during the boreal spring, early summer, and fall coinciding with the active period of the Wyrtki Jet, a surface-intensified eastward-flowing current observed in the equatorial Indian Ocean during the monsoon transitions (Wyrtki, 1973). Previous mooring measurements show that the Wyrtki jet can extend to greater than 900 m depth and reach northward beyond 5° N (Reppin et al., 1999).

The mechanisms driving the undercurrent are still unclear, but they are likely to vary at different times of the year. A Hovmöller diagram of POP meridional velocity across 8° N (Figure 5) shows the westward propagation of the velocity signal at 729 m depth originating from the eastern boundary of the BoB that takes about four months to cross the southern BoB. This provides a propagation speed of 12 cm s^{-1} which is in good agreement with the phase speed of a mode 2 baroclinic Rossby wave in this region (Shankar et al., 1996; Killworth and Blundell, 2003). A westward-propagating southward current begins to develop at the eastern boundary of the BoB in April-May and reaches the east coast of Sri Lanka in September contributing to the observed southward-flowing subsurface current (Figure 3 and Figure 5); this is consistent with findings from a stratified linear model study (McCreary et al., 1996). Even though the Rossby waves do not directly influence the undercurrent observed during spring and summer, it might be important in setting up the spring undercurrent; the influence of Rossby waves on the undercurrent is still unclear and more studies are needed. The westward propagating northward and southward flows originating at 83° E-85° E in April (Figure 5b) are associated with the subsurface anticyclonic eddy observed along the east coast of Sri Lanka during the summer (Figure 4b).

The stratified linear model study (McCreary et al., 1996) also indicates the role of Ekman pumping in producing the undercurrent. The model suggests that Ekman pumping induces the undercurrent during the boreal spring and summer; the undercurrent with its core at 400-500 m can reach a maximum speed of 10 cm s^{-1} southward and northward in March-April and August respectively. This agrees quite well with the spring undercurrent observed in the observations and OGCMs (Figure 3).

To estimate the role of the undercurrent in the exchange of salt between the BoB and the rest of the northern Indian Ocean basin, we calculated the salt transport resulting from the reversing undercurrent. The time series of salinity averaged over the width of the undercurrent (from the east coast of Sri Lanka to 82.5° E) from POP and the volume transport of the POP undercurrent (over 200-1000 m) along 8° N are shown in Fig. 6. The time series clearly shows fresh water flowing southward and salty water flowing northward with a correlation coefficient of 0.50 that is significant at the 95% confidence level.

Ocean Sci. Discuss., https://doi.org/10.5194/os-2017-38
Manuscript under review for journal Ocean Sci.
Discussion started: 11 July 2017

The salt transport due to the fluctuations of the flow and of the salinity (departures from the 13-year climatology) in the 200-1000 m layer is 0.04×10^6 kg s^{-1}. This is only 1% of the total expected salt transport into the BoB of $4.5\text{-}4.9\times10^6$ kg s^{-1} estimated from an expected annual freshwater input of 0.13-0.14 Sv (Rao and Sivakumar, 2003; Sengupta et al., 2006; Wilson and Riser, 2016). Note that the total net salt transported in POP into the BoB across 8° N is 4.3×10^6 kg s^{-1} which is in good agreement with the previously reported values. Estimates of salt flux by the mean flow over the same depth layer from POP and HYCOM are even smaller: the mean undercurrent transport of 1.5-2 Sv in the OGCMs is fresher than the interior northward flow as judged from HYCOM and sparse CTD and Argo profiles (not shown), but the salinity contrast at this depth layer is very small. In addition, the small salt transport from the mean flow in the 200-1000 m layer might be due to the core of the undercurrent moving vertically such that this layer may sometimes include opposite flows or smaller salinity contrasts with the interior (Figure 3).

Compared to observations of other low-latitude western boundary undercurrents, e.g. the Mindanao Undercurrent (MUC) in the Pacific Ocean, the undercurrent along the east coast of Sri Lanka exhibits many similar physical properties. Both undercurrents span over 400 m to a depth greater than 1000 m. The MUC core is located between 500-950 m with a maximum mean speed of 10-20 cm s^{-1} (Hu et al., 1991; Zhang et al., 2014) and the undercurrent along the Sri Lankan east coast has its core between 300-800 m with a maximum mean speed of 15-30 cm s^{-1} (Figure 3). However, the MUC is narrower, about 50 km wide. Also, the MUC does not exhibit distinct seasonal variation (Qu et al., 2012; Hu et al., 2016), while the undercurrent along the Sri Lankan east coast reverses its direction seasonally. Both Ekman pumping and Rossby waves are important in modifying the MUC (Qu et al., 2012; Chiang and Qu, 2013; Zhang et al., 2014; Hu et al., 2016). While Ekman pumping is likely to have significant impact on the undercurrent along the Sri Lankan east coast, the role of Rossby waves is still unclear.

5 Summary

The velocity fields derived from CTD and Argo profiles, glider measurements, POP, and HYCOM reveal the presence of an undercurrent off the east coast of Sri Lanka that reverses seasonally. The OGCMs also suggest active salt transport along the east coast of Sri Lanka by the undercurrent. Salt transport across 8° N by the fluctuating undercurrent estimated from POP contributes about 1%, and the transport by the mean undercurrent estimated from HYCOM is under 0.1% of the expected total salt input into the BoB. The mechanisms driving the undercurrent are still unclear, though Ekman pumping is likely to affect the undercurrent especially during the boreal spring (McCreary et al., 1996). Our analyses do not observe the direct influence of Rossby waves on the modification of the undercurrent, but they might have a crucial role in setting up the southward-flowing spring undercurrent. Understanding the role and driving mechanisms of the undercurrent can potentially, in turn, provide a better understanding of what drives the contrasting salinity distribution in the northern Indian Ocean.

Acknowledgements

This work is supported by the US Office of Naval Research (ONR) as part of two ONR Departmental Research Initiatives: Air-Sea Interactions Regional Initiative (ASIRI) and Northern Arabian Sea Circulation – autonomous research (NASCar) projects through ONR grants N00014-14-1-0629 (A. Anutaliya and U. Send), N00014-15-1-2189 (J. L. McClean), N00014-16-1-2313 (J. Sprintall), N00014-13-1-0478, N00014-15-1-2296, N00014-15-1-2231 (L. Rainville and C. Lee). J. Metzger and A. Wallcraft are supported by the Eddy resolving global ocean prediction including tides project under ONR program element 0602435N. CTD profiles are from the National Center of Environmental Information (Boyer et al., 2013) (https://www.nodc.noaa.gov/access/index.html). Argo data were collected and made freely available by the International Argo Program and the national programs that contribute to it (http://www.argo.ucsd.edu, http://argo.jcommops.org). The Argo Program is part of the Global Ocean Observing System. The altimeter products were produced by Ssalto/Duacs and distributed Aviso, with support from Cnes (http://www.aviso.altimetry.fr/duacs/). The HYCOM simulation was performed using grants of computer time from the Department of Defense High Performance Computing Modernization Program. This is NRL contribution NRL/JA/7320-17-3395, which is approved for public release and distribution is unlimited. The POP simulation was carried out using the Extreme Science and Engineering Discovery Environment (XSEDE), which is supported by National Science Foundation grant number ACI-1548562. POP output is available from XSEDE. Thanks to He Wang (SIO) for helpful discussions about the salt transport calculation. Also, thanks to Judy Gaukel (SIO) for extracting and transferring the OGCM files.

References

Boyer, T.P., J. I. Antonov, O. K. Baranova, C. Coleman, H. E. Garcia, A. Grodsky, D. R. Johnson, R. A. Locarnini, A. V. Mishonov, T.D. O'Brien, C.R. Paver, J.R. Reagan, D. Seidov, I. V. Smolyar, and M. M. Zweng, (2013), World Ocean Database 2013, NOAA Atlas NESDIS 72, S. Levitus, Ed., A. Mishonov, Technical Ed.; Silver Spring, MD, 209 pp., http://doi.org/10.7289/V5NZ85MT

Chiang, T.-L., and T. Qu (2013), Subthermocline eddies in the western equatorial Pacific as shown by an eddy-resolving OGCM. J. Phys. Oceanogr., 43, 1,241-1,253, doi:10.1175/JPO-D-12-0187.1.

de Vos, A., C. B. Pattiaratchi, and E. M. S. Wijeratne (2014), Surface circulation and upwelling patterns around Sri Lanka. Biogeosciences, 11, 5,905-5,930. doi:10.5194/bg-11-5909-2014.

Delman, S. A., J. L. McClean, J. Sprintall, L. D. Talley, E. Yulaeva, and S. R. Jayne (2015), Effects of Eddy Vorticity Forcing on the Mean State of the Kuroshio Extension. J. Phys. Oceanogr., 45, 1,356–1,375.

Ducet, N., P. Y. L. Traon, and G. Reverdin (2000), Global high-resolution mapping of ocean circulation from TOPEX/Poseidon and ERS-1 and -2. J. Geophys. Res., 105, 19,477-19,498.

Durand, F., D. Shankar, F. Birol, and S. S. C. Shenoi (2009), Spatiotemporal structure of the East India Coastal Current from satellite altimetry. J. Geophys. Res., 114, C02013, doi:10.1029/2008JC004807.

Gordon, A. L., E. L. Shroyer, A. Mahadevan, D. Sengupta, and M. Freilich (2016), Bay of Bengal: 2013 northeast monsoon upper-ocean circulation. Oceanography, 29(2), 82-91, http://dx.doi.org/10.5670/oceanog.2016.41.

Hacker, P., E. Firing, and J. Hummon (1998), Bay of Bengal currents during the northeast monsoon. Geophys. Res. Lett., 25(15), 2,769-2,772, doi:10.1029/98GL52115.

Hu, D., M. Cui, T. Qu, and Y. Li (1991), A subsurface northward current off Mindanao identified by dynamic calculation. Oceanogr. Asian Marginal Seas-Elsevier Oceanogr. Ser., 54, 359-365, doi:10.1016/S0422-9894(08)70108-9.

Hu, S., D. Hu, C. Guan, F. Wang, L. Zhang, F. Wang, and Q. Wang (2016), Interannual Variability of the Mindanao Current/ Undercurrent in Direct Observations and Numerical Simulations. J. Phys. Oceanogr., 46, 483-499.

Jensen, T.G., H. W. Wijesekera, E. S. Nyadjro, P. G. Thoppil, J. F. Shriver, K. K. Sandeep, and V. Pant (2016), Modeling salinity exchanges between the equatorial Indian Ocean and the Bay of Bengal. Oceanography, 29(2), 92-101, http://dx.doi.org/10.5670/oceanog.2016.42.

Killworth, P. D., and J. R. Blundell (2003), Long extratropical planetary wave propagation in the presence of slowly varying mean flow and bottom topography. Part I: The local problem. J. Phys. Oceanogr., 33, 784-801.

Lee, C. M., S. U. P. Jinadasa, A. Anutaliya, L. R. Centurioni, H. J. S. Fernando, V. Hormann, M. Lankhorst, L. Rainville, U. Send, and H. W. Wijesekera (2016), Collaborative observations of boundary currents, water mass variability, and monsoon response in the southern Bay of Bengal. Oceanography, 29(2), 102–111, http://dx.doi.org/10.5670/oceanog.2016.43.

McCreary, J. P., W. Han, D. Shankar, and S. R. Shetye (1996), Dynamics of the East India Coastal Current 2. Numerical solutions. J. Geophys. Res., 101, 13,993-14,010, doi:10.1029/96JC00560.

Metzger, E. J., H. E. Hurlburt, X. Xu, J. F. Shriver, A. L. Gordon, J. Sprintall, R. D. Susanto, H. M. van Aken (2010), Simulated and observed circulation in the Indonesian Seas: 1/12o global HYCOM and the INSTANT observations. Dyn. Atmos. Oceans, 50, 275-300, doi:10.1016/j.dynatmoce.2010.04.002.

Maltrud, M. E., F. O. Bryan, and S. Peacock (2010), Boundary impulse response functions in a century-long eddying global ocean simulation. Environ. Fluid Mech., 10, 275-295, doi:10.1007/s10652-009-9154-3.

Qu, T., T. L. Chiang, C. R. Wu, P. Dutrieux, and D. Hu (2012), Mindanao Current/ Undercurrent in an eddy-resolving GCM. J. Geophys. Res., 117, C06026, doi:10.1029/2011JC007838.

Rao, R. R., R. Sivakumar (2003), Seasonal variability of sea surface salinity and salt budget of the mixed layer of the north Indian Ocean. J. Geophys. Res. Oceans, 108(C1), 9-1 – 9-14, doi:10.1029/2001JC00907.

Reppin, J., F. A. Schott, and J. Fischer (1999), Equatorial currents and transports in the upper central Indian Ocean: Annual cycle and interannual variability. J. Geophys. Res., 104(C7), 15,495-15,514.

Rosmond, T. E., J. Teixeira, M. Peng, T. F. Hogan, and R. Pauley (2002), Navy Operational Global Atmospheric Prediction System (NOGAPS): forcing for ocean models. Oceanography, 15(1), 99-108.

Sengupta, D., G. N. Bhsrath Raj, S. S. C. Shenoi (2006), Surface freshwater from Bay of Bengal runoff and Indonesian Throughflow in the tropical Indian Ocean. Geophys. Res. Lett., 33(22), L22609, doi:10.1029/2006GL027573.

Shankar, D., J. P. McCreary, and W. Han (1996), Dynamics of the East India Coastal Current 1. Analytic solutions forced by interior Ekman pumping and local alongshore winds. J. Geophys. Res., 101(C6), 13,975-13,991.

Shetye, S. R., A. D. Gouveia, S. S. C. Shenoi, D. Sundar, G. S. Michael, and G. Nampoothiri (1993), The western boundary current of the seasonal subtropical gyre in the Bay of Bengal. J. Geophys. Res., 98(C1), 945-954.

Shetye, S. R., A. D. Gouveia, D. Shankar, S. S. C. Shenoi, P. N. Vinayachandran, D. Sundar, G. S. Michael, and G. Nampoothiri (1996), Hydrography and circulation in the western Bay of Bengal during the northeast monsoon. J. Geophys. Res., 101, 14,011-14,025.

Smith, R., P. Jones, B. Briegleb, F. Bryan, G. Danabasoglu, J. Dennis, J. Dukowicz, C. Eden, B. Fox-Kemper, P. Gent, M. Hecht, S. Jayne, M. Jochum, W. Large, K. Linday, M. Maltrud, N. Norton, S. Peacock, M. Vertenstein, and S. Yeager (2010), The Parallel Ocean Program (POP) reference manual. LANL/NCAR Tech. Rep. LAUR-10-01853, 140 pp.

Vinayachandran, P. N., and T. Yamagata (1997), Monsoon response of the sea around Sri Lanka: generation of thermal domes and anticyclonic vortices. J. Phys. Oceanogr., 28, 1,946-1,960.

Vinayachandran, P. N., Y. Masumoto, T. Mikawa, and T. Yamagata (1999), Intrusion of the southwest monsoon current into the Bay of Bengal. J. Geophys. Res., 104(C5), 11,077-11,085.

Vinayachandran, P. N., D. Shankar, S. Vernekar, K. K. Sandeep, P. Amol, C. P. Neema, and A. Chatterjee (2013), A summer monsoon pump to keep the Bay of Bengal salty. Geophys. Res. Lett., 40, 1777-1782, doi:10.1002/grl.50274.

Wilson, E. A., S. C., Riser (2016), An Assessment of the Seasonal Salinity Budget for the Upper Bay of Bengal. J. Phys. Oceanogr., 46, 1,361-1,376.

Wijesekera, H. W., T. G. Jensen, E. Jarosz, W. J. Teague, E. J. Metzger, D. W. Wang, S. U. P. Jinadasa, K. Arulananthan, L.R. Centurioni, and H. J. S. Fernando (2015), Southern Bay of Bengal currents and salinity intrusions during the northeast monsoon. J. Geophys. Res. Oceans, 120, 6,897-6,913, doi:10.1002/2015JC010744.

Wyrtki, K. (1973), An Equatorial Jet in the Indian Ocean. Science, 181, 262-264.

Yu, L., J. J. O'Brien, and J. Yang (1991), On the Remote Forcing of the Circulation in the Bay of Bengal. J. Geophys. Res., 96, 20,449-20,454.

Zhang, L., D. Hu, S. Hu, F. Wang, F. Wang, and D. Yuan (2014), Mindanao Current/ Undercurrent measured by a subsurface mooring. J. Geophys. Res. Oceans, 119, 3,617-3,628, doi:10.1002/2013JC009693.

Ocean Sci. Discuss., https://doi.org/10.5194/os-2017-38
Manuscript under review for journal Ocean Sci.
Discussion started: 11 July 2017

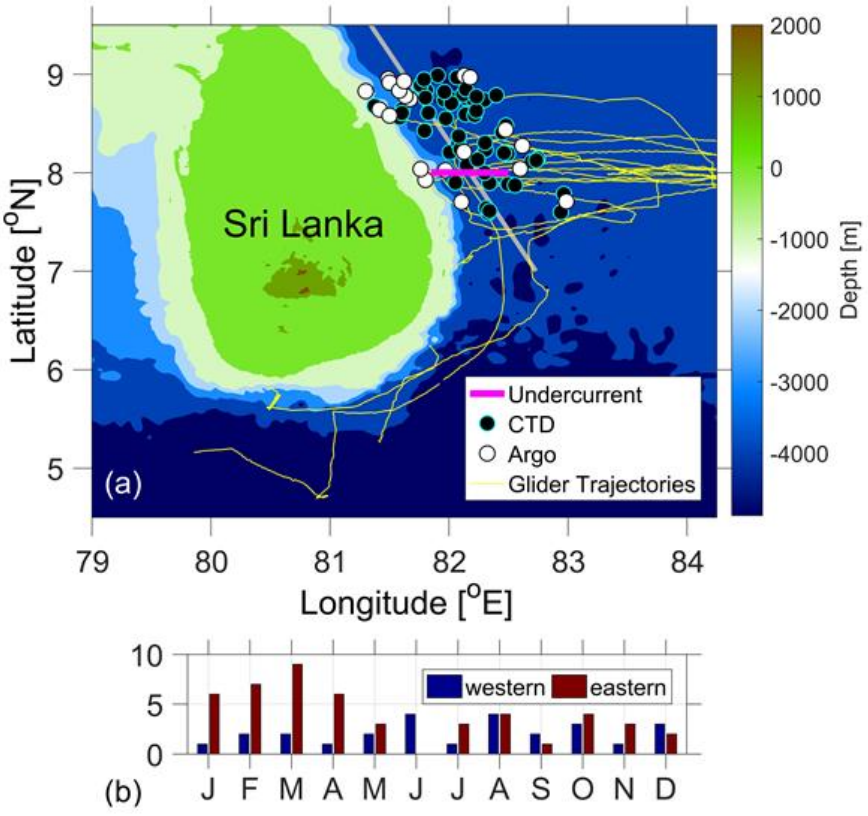

Figure 1: Bathymetry around Sri Lanka (a) with the location of the CTD measurements (black dots), Argo profiles (white dots), and glider measurement transects (yellow lines). The gray line divides CTD and Argo measurements into the eastern and western halves used in the seasonal mean dynamic height calculation. The OGCM outputs are interpolated along 8° N (magenta line). The number of CTD and Argo profiles available in the mean dynamic height calculation for each month for the eastern (red) and western (blue) halves are shown in (b).

Ocean Sci. Discuss., https://doi.org/10.5194/os-2017-38
Manuscript under review for journal Ocean Sci.
Discussion started: 11 July 2017

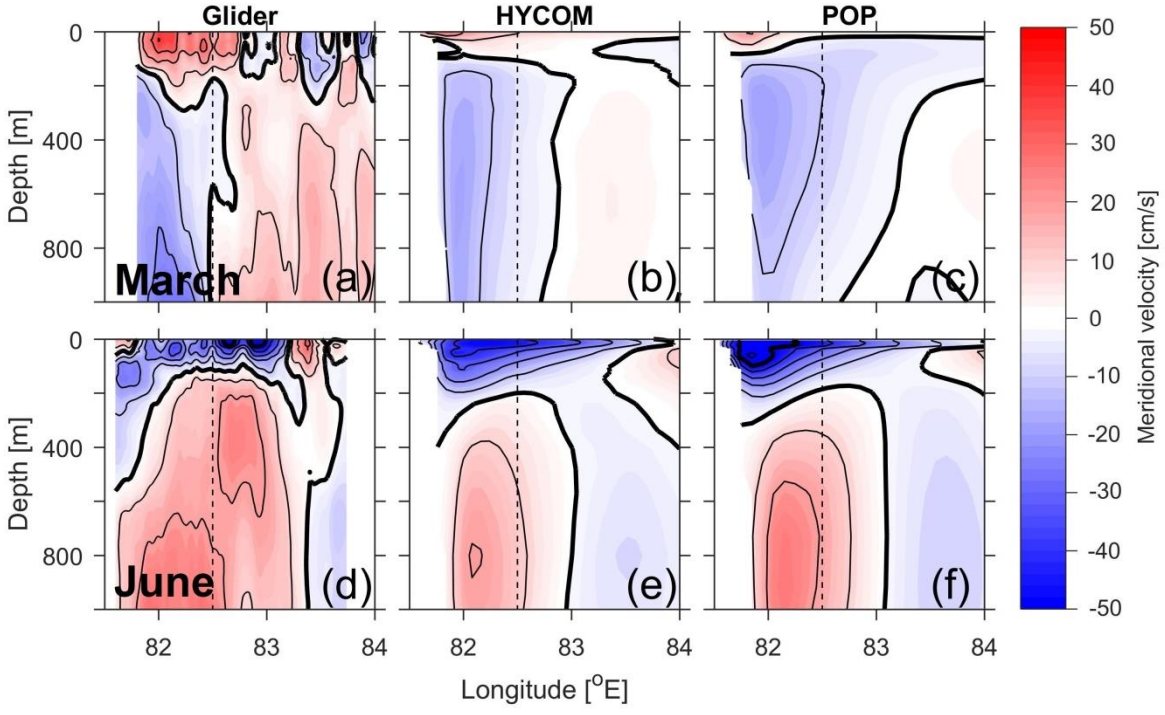

Figure 2: Absolute geostrophic meridional velocity across 8° N measured by gliders during March 18-30, 2014 (a) and May 24 – Jun 8, 2014 (d), the mean meridional velocity from HYCOM (b and e) and POP (c and f) in March and June over 2003-2012 and 1995-2007 periods respectively. The black dashed line marks the eastern boundary of the undercurrent. Thin black lines are plotted every 10 cm s^{-1}, and thick black lines are plotted every 50 cm s^{-1}.

Ocean Sci. Discuss., https://doi.org/10.5194/os-2017-38
Manuscript under review for journal Ocean Sci.
Discussion started: 11 July 2017

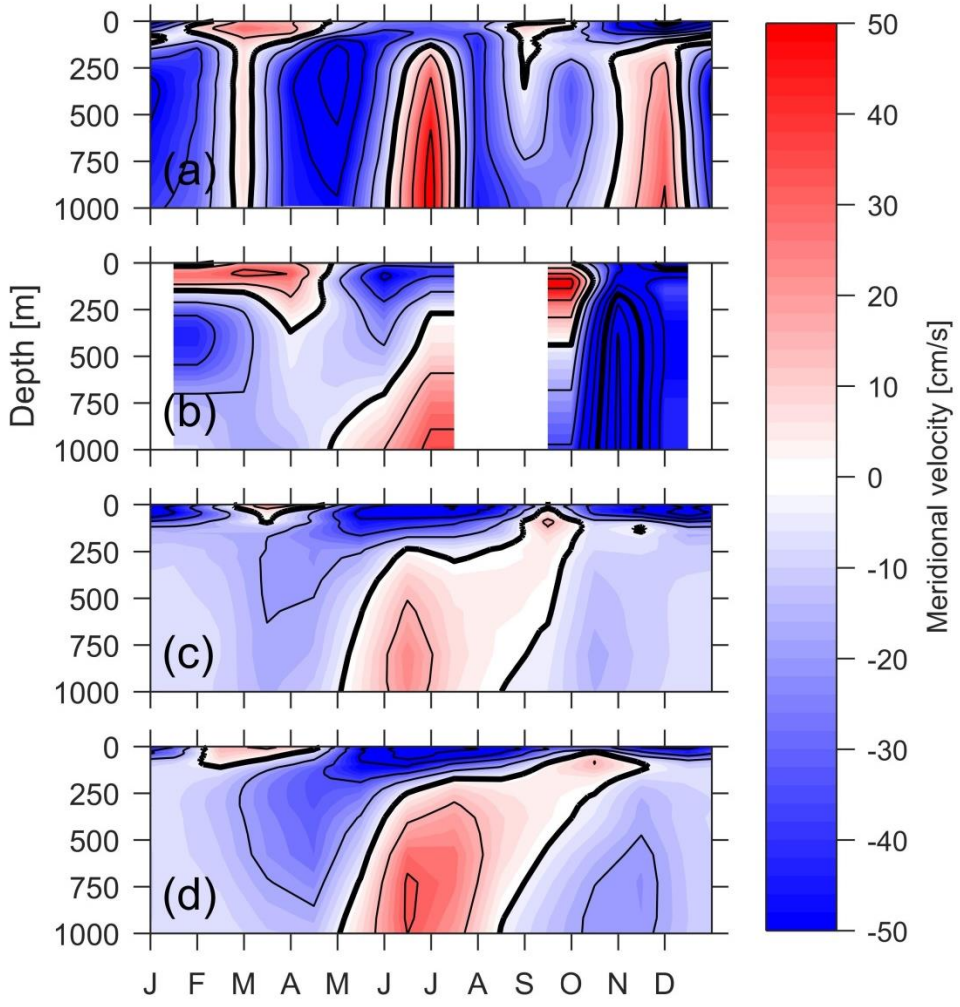

Figure 3. Bimonthly sliding mean seasonal variation of the meridional geostrophic velocity profiles derived from CTD and Argo measurements (a), glider measurements (b), and monthly mean meridional velocity profiles averaged across the magenta transect shown in Fig. 1 from HYCOM (c), and POP outputs (d). Line contours are plotted in the same manner as in Fig. 2.

Ocean Sci. Discuss., https://doi.org/10.5194/os-2017-38
Manuscript under review for journal Ocean Sci.
Discussion started: 11 July 2017

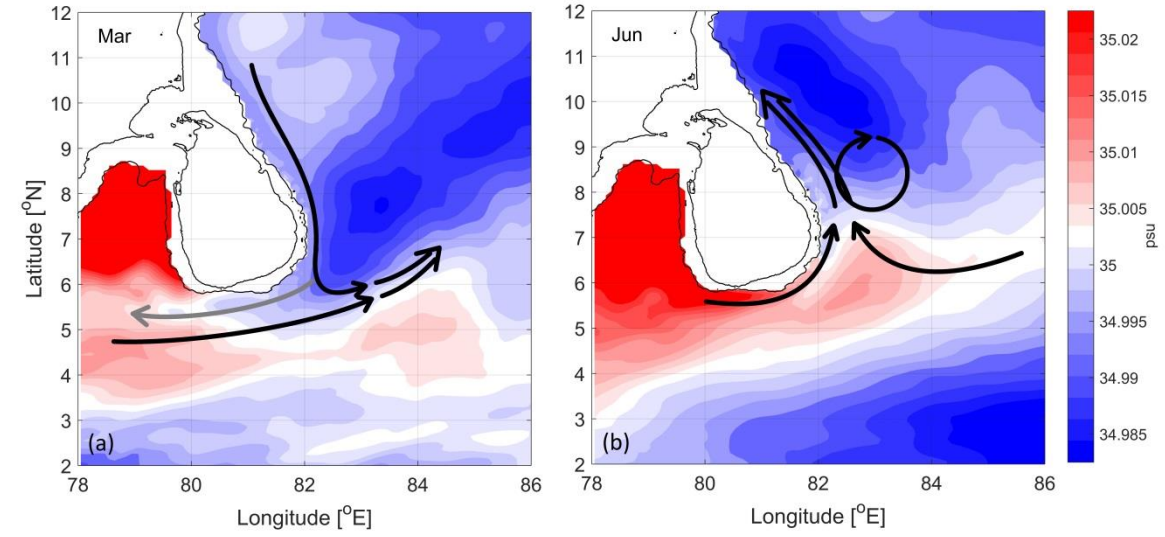

Figure 4. Simplified schematic of the undercurrent along the east and south coast of Sri Lanka at 729 m depth based on POP outputs in March (a) and June (b) plotted over corresponding POP monthly mean salinity. The black arrows represent the current pattern at 729 m that reoccurs every year, and the gray arrow shows circulation that is observed only in some years. The 0 and 1000 m bathymetry contours are plotted as thin black lines.

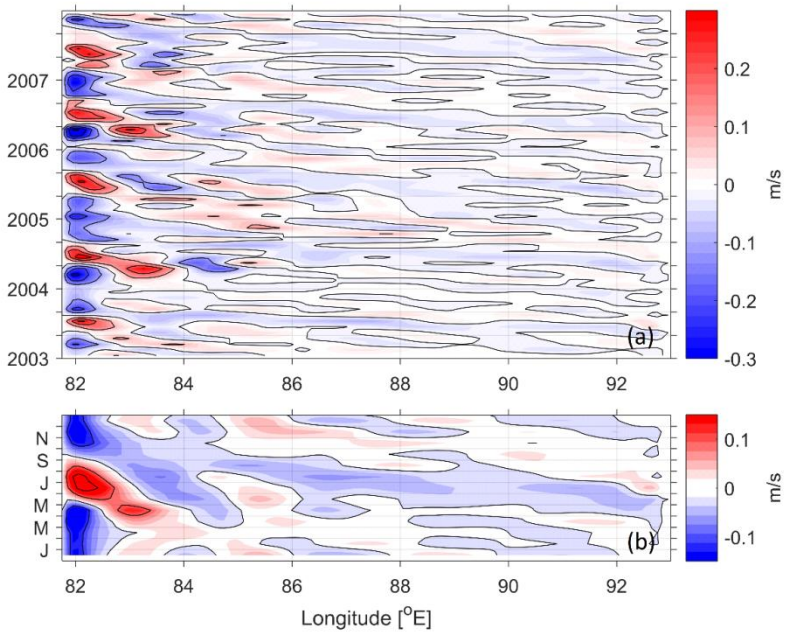

Figure 5. Time-longitude plots of monthly meridional velocity (a) and seasonal mean velocity (b) over 2003-2007 across 8° N at 729 m from POP.

Ocean Sci. Discuss., https://doi.org/10.5194/os-2017-38
Manuscript under review for journal Ocean Sci.
Discussion started: 11 July 2017

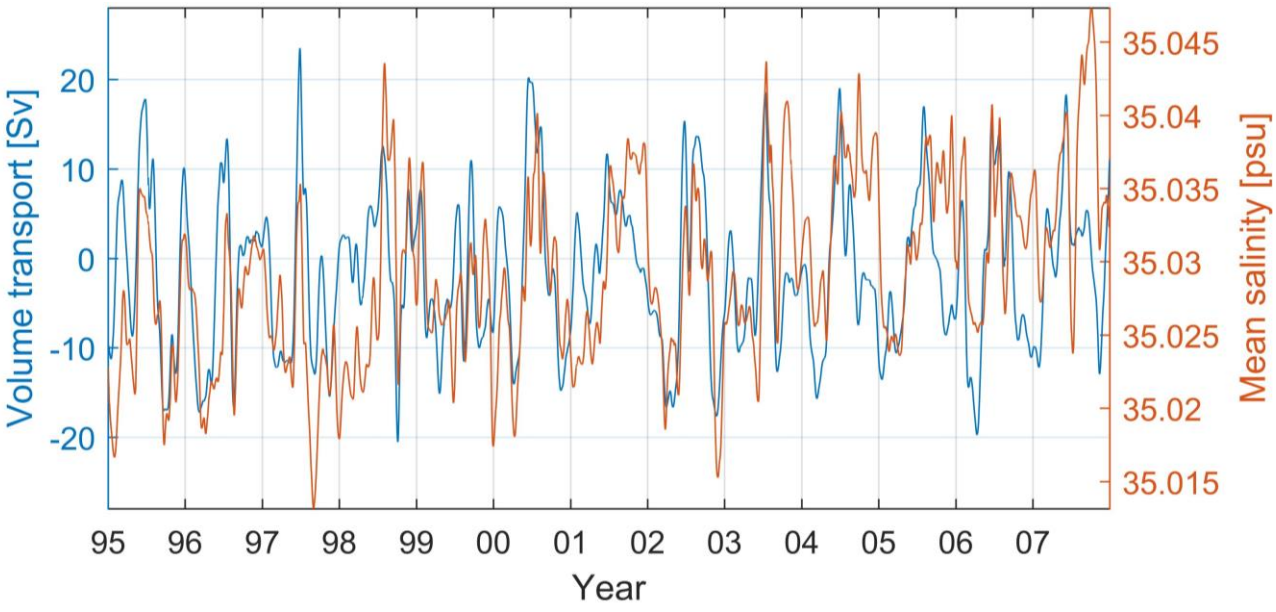

Figure 6. Time series of volume transport and mean salinity between 81.5° E and 82.4° E in the 200-1000 m layer from POP.